FLAGCAL: Imaging Results

Dharam Vir LAL
dharam AT ncra DOT tifr DOT res DOT in

February 7, 2014

Contents

List of Figures

List of Tables

1 Overview

This documents summarises imaging results from the FLAGCAL [1] (all FLAGCAL releases prior to ver. 0.989). The effectiveness of low frequency observations has been limited due to four main reasons: (i) the low resolution, (ii) sidelobe confusion from bright outlier sources, (iii) the ionosphere-induced phase distortions, and (iv) man-made radio frequency interference (RFI). FLAGCAL attempts to correct corruptions due to RFI and instrumental errors giving an output that is a calibrated and flagged FITS file, which can be directly used for imaging and further processing. Several GMRT data sets were reduced at various low radio frequencies ($<$ 1.4 GHz), both via manual data analyses and via FLAGCAL for a faithful comparison. Here we present results from these exercises.

This report is organized as follows. Section 1.1 contains our rationale towards the choice of various GMRT data from the archive. Results of the data analysis are presented in subsequent sections, namely, Section 1.2 showing flux density scales; Section 1.3.1, 1.3.2, 1.3.3 and 1.3.4 show imaging results at 610 MHz, 325 MHz, 240 MHz and 150 MHz respectively. The comparisons of peak surface brightness, RMS, etc. from the manually reduced images and the FLAGCAL images at these frequencies are given in Table 2. We summarise our findings in Section 1.4 and make some final concluding remarks.

1.1 Data

GMRT data for several targets were extracted from the GMRT archive. The choice of the data was radom to some extent, but it was also based on my scientific interests. Nevertheless, several fields ranging from point source dominated to extended source dominated fields were mapped. The observing log for all the imaged fields is shown in Table 1.

Table 1: GMRT observations analysed in this report.

	Obs ID	Frequency	Obs. Date	Target
Flux density scales	17_034	610 MHz	2010-02-13	1311−222
		240 MHz	2010-01-24	1311−222
	13SPA01	325 MHz	2008-01-02	3C 452
	08MHa01	610 MHz	2005-06-18	3C 382
		610 MHz	2005-05-31	3C 321
		610 MHz	2005-06-17	3C 33
		240 MHz	2005-06-17	3C 33
Imaging	23_046	610 MHz	2012-10-20	Abell 3411
	03DVL02	610 MHz	2002-12-21	NGC 1265
	22_029	610 MHz	2012-09-15	Abell 2552
	23_46	325 MHz	2012-11-18	Abell 3411
	17_034	325 MHz	2010-02-18	NGC 5044
	13SPA01	325 MHz	2008-01-02	3C 452
		240 MHz		0702+5002
	17_034	240 MHz	2010-02-14	NGC 5044
	08HRa01	150 MHz	2005-05-20	Abell 2256

[1] FLAGCAL: http://ncralib1.ncra.tifr.res.in:8080/jspui/handle/2301/581

1.2 Flux density scales

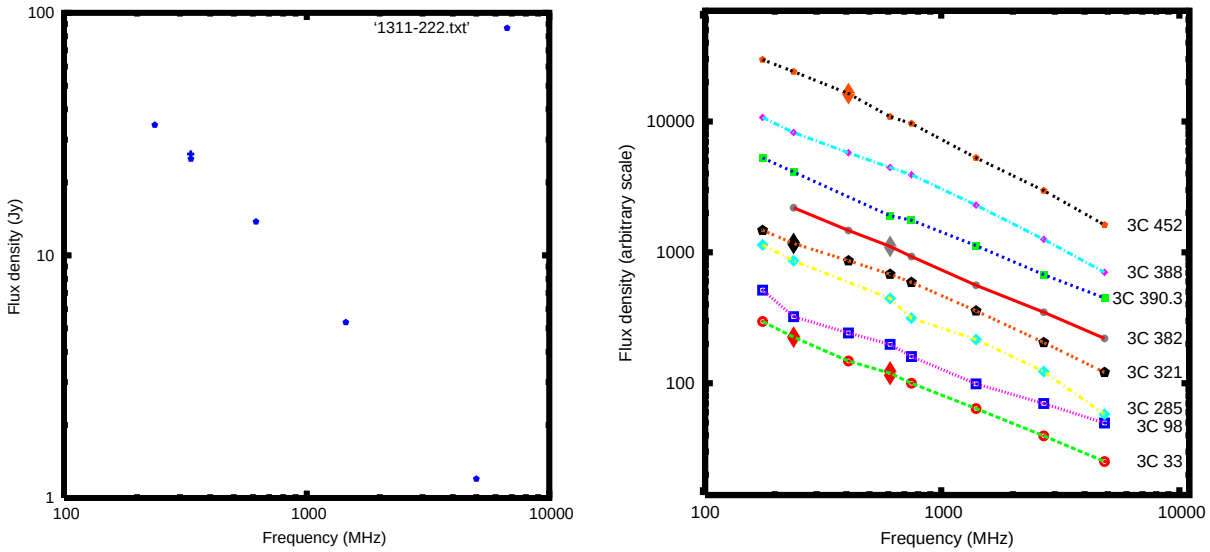

Figure 1: Plot showing flux density as a function of frequency. Left panel shows the values of flux density at 610, 325 and 240 MHz for a calibrator source 1311−222 using FLAGCAL. The flux densities at L-band and at the P-band were plotted from the VLA calibrator manual. Right panel shows the integrated flux densities spectra for a few of the 3C radio galaxies using FLAGCAL from a sample of sources compiled by Lal et al. (2008) at 610, 325 and 240 MHz, which are plotted using 'Diamond' symbols. The spectra are shifted with respect to one another for clarity.

To establish the flux density scales, GMRT data for the calibrator source B1311−222 was analysed using FLAGCAL at 240 MHz, 325 MHz and 610 MHz. The flux density scales for the primary calibrator sources (3C 48, 3C 147 and 3C 286) were set by Perley & Taylor (1999) extension to Baars et al. (1977) scale. The data (plotted in Fig. 1, left panel) was consistent with

$$s_\nu \propto \nu^{-\alpha}$$

where α = 1.03 $\pm$0.03. The flux densities at L-band and at P-band were plotted from the VLA calibrator manual[2].

To further establish the flux density scales, the GMRT archive data for 3C 452 at 325 MHz, 3C 382 at 610 MHz, 3C 321 at 240 MHz, and 3C 33 at 240 MHz and at 610 MHz were analysed using FLAGCAL. The integrated flux densities spectra were plotted along with the sample of 'Normal' Fanaroff-Riley type II 3C radio galaxies compiled by Lal et al. (2008)[3]. The error bars (not plotted) on various measurements are typically either smaller than the symbol sizes or two times the symbol sizes. The spectra are shifted with respect to one another for clarity.

[2]VLA calibrator manual: http://www.vla.nrao.edu/astro/calib/manual/

[3]Lal et al. 2008 MNRAS 390, 1105

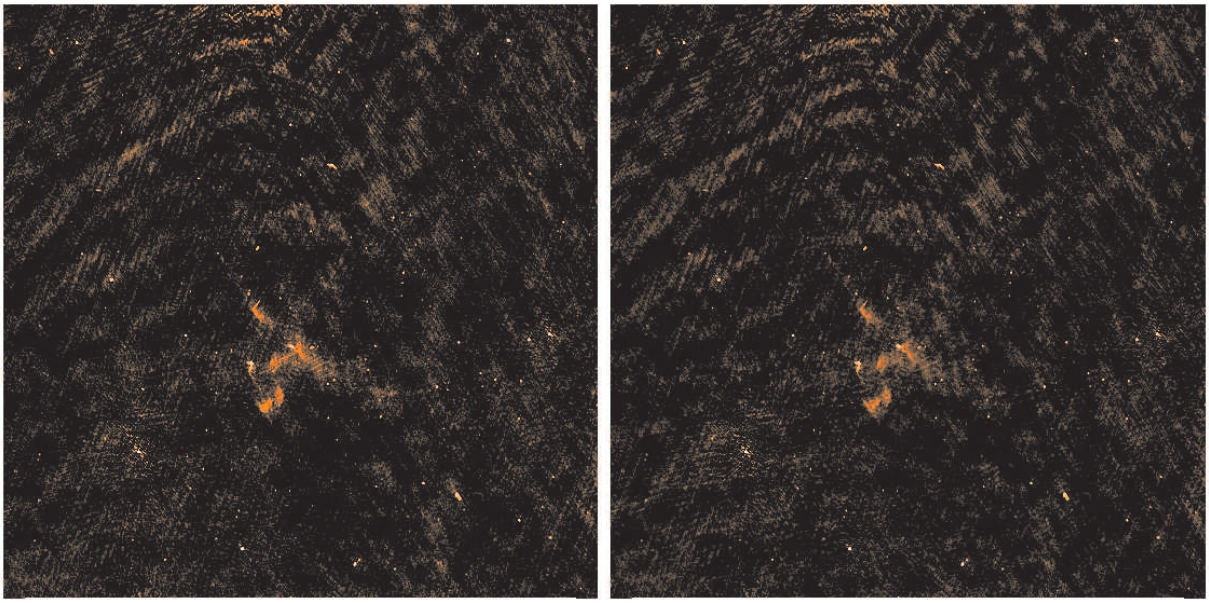

Figure 2: Image of Abell 3411 at 610 MHz obtained via two methods. The left panel is manually reduced image and the right panel is FLAGCAL image.

1.3 Imaging

1.3.1 610 MHz

The imaging results at 610 MHz for Abell 3411 and for NGC 1265 sources are presented in Fig. 2 and in Fig. 3, respectively. Remarkable morphological agreements seen in both fields are worth noting. Abell 3411 is a galaxy cluster undergoing a merger event. Both images, FLAGCAL image and the manually reduced image, show the presence of large-scale, complex-shaped, diffuse emission in the central region of the cluster, possibly a radio halo. Images of the head-tail radio galaxy NGC 1265 also show remarkable morphological similarities. Both images also show presence of a nuclear component, several bright spots tracing most of the way from the nucleus out into the more diffuse structure which makes the radio tail. The peak flux densities of the unresolved nuclear source matches well (within errorbars) in the two images.

As an independent check, another data for Abell 2552 was analysed using FLAGCAL and manually by Dr. R. Kale. Once again both images in Fig. 4 show morphological agreements and positional agreements with uncertainties, and agreements in peak flux densities and RMS noise levels in the two methods.

1.3.2 325 MHz

The imaging results at 325 MHz for NGC 5044 and 3C 452 sources are presented in Fig. 5 and Fig. 6, respectively. We intentionally chose NGC 5044 field so as to compare morphological details seen in the 610 MHz. The presence of large-scale, complex-shaped, diffuse emission in the central region of the cluster is clearly seen in the 325 MHz image, which was also seen in the 610 MHz images, providing us with immense confidence in FLAGCAL.

3C 452 is a Fanaroff-Riley type II radio galaxy. Morphologically, the total angular extent (1×4 arcmin^2) is identical in both images. The position of the nucleus agree within the positional uncertainties of the two images. As shown in Fig. 1, the spectra of 3C 452 of determined from the integrated flux densities is seen to be a classical straight spectra.

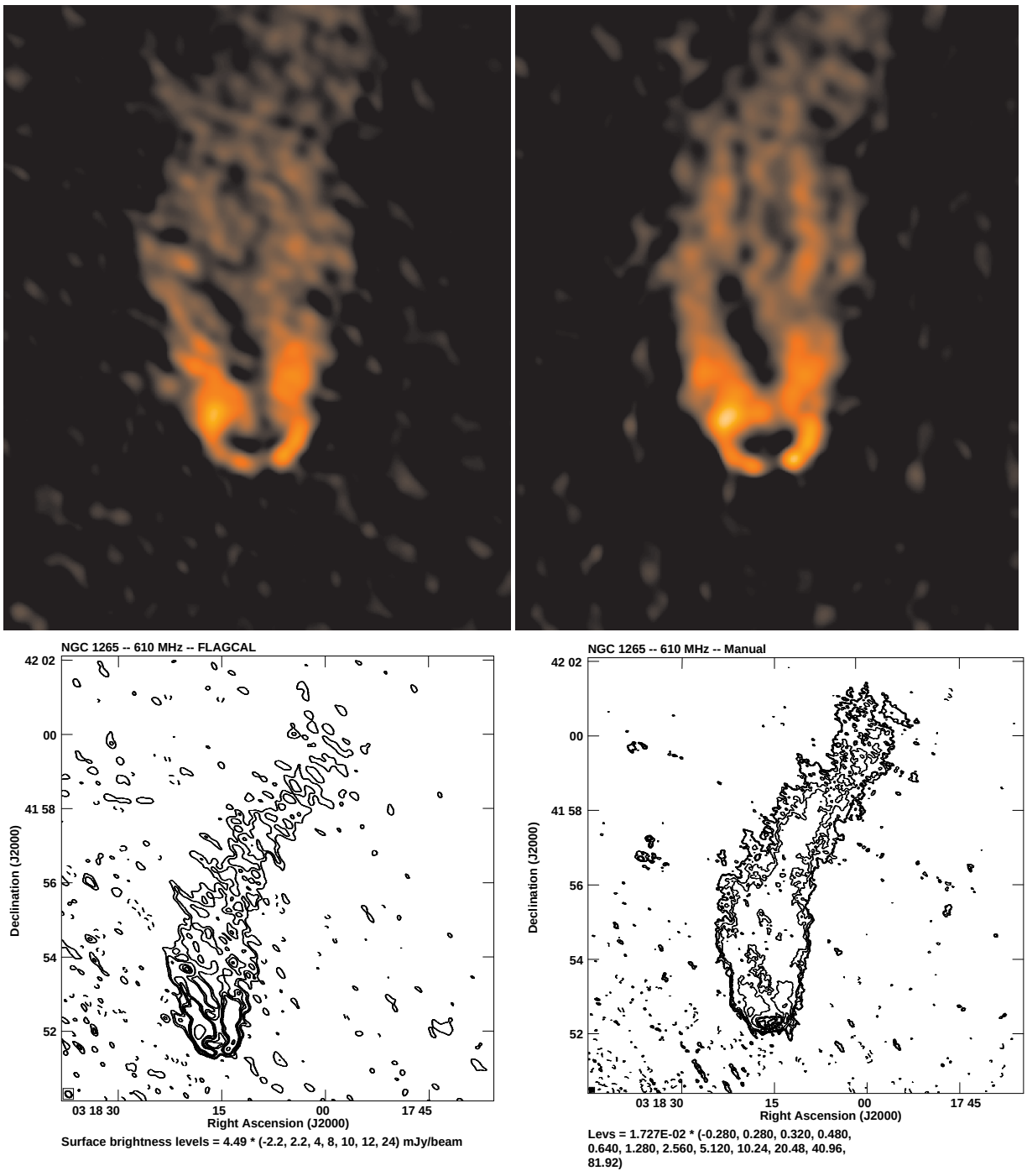

Figure 3: Image of NGC 1265 at 610 MHz obtained via two methods. In both, upper and lower panels, the left panel images are from FLAGCAL data analysis and the right panel images are from the manual data analysis.

Table 2: Table showing a few figures of merit from the imaging results obtained from the two methods. Except source 0702+5002, where the results are from dirty image, results for the rest are based on the respective CLEAN images. (Abell 2552, credits: Dr. R. Kale.)

			manual	FLAGCAL
610 MHz	Abell 3411	peak	28.7 mJy	29.4 mJy
		RMS	91 μJy beam^{-1}	120 μJy beam^{-1}
		beam	5.5 $\times$ 4.8 arcsec^2	5.6 $\times$4.8 arcsec^2
	NGC 1265	peak	89.7 mJy	76.9 mJy
		RMS	7.18 mJy beam^{-1}	3.75 mJy beam^{-1}
		beam	5.8 $\times$ 4.9 arcsec^2	6.0 $\times$ 4.5 arcsec^2
	Abell 2552	peak	52.0 mJy	49.3 mJy
	(Credits: Dr. R. Kale)	RMS	$\sim$35 μJy beam^{-1}	$\sim$35 μJy beam^{-1}
		beam	$\sim$6.0 $\times$ 4.0 arcsec^2	$\sim$6.0 $\times$ 4.0 arcsec^2
325 MHz	3C 452	peak	1.39 Jy	1.43 Jy
		RMS	10.82 mJy beam^{-1}	13.92 mJy beam^{-1}
		beam	22.4 $\times$ 19.7 arcsec^2	22.4 $\times$ 19.9 arcsec^2
	Abell 3411	peak	9.42 mJy	9.15 mJy
		RMS	0.23 mJy beam^{-1}	0.27 mJy beam^{-1}
		beam	10.2 $\times$ 8.0 arcsec^2	10.5 $\times$ 8.1 arcsec^2
	NGC 5044	peak	0.37 mJy	0.29 mJy
		RMS	0.57 mJy beam^{-1}	0.51 mJy beam^{-1}
		beam	10.0 $\times$ 9.3 arcsec^2	11.2 $\times$ 9.9 arcsec^2
240 MHz	0702+5002	peak	2.27 Jy	2.19 Jy
	(dirty image)	RMS	10.1 mJy beam^{-1}	10.5 mJy beam^{-1}
		beam	18.5 $\times$ 11.4 arcsec^2	18.7 $\times$ 12.6 arcsec^2
	NGC 5044	peak	1.45 Jy	1.36 Jy
		RMS	2.9 mJy beam^{-1}	1.9 mJy beam^{-1}
		beam	20.1 $\times$ 17.4 arcsec^2	14.7 $\times$ 12.9 arcsec^2
150 MHz	Abell 2256	peak	0.14 Jy	0.33 Jy
		RMS	4.2 mJy beam^{-1}	18.0 mJy beam^{-1}
		beam	23.3 $\times$ 20.1 arcsec^2	27.6 $\times$ 24.6 arcsec^2

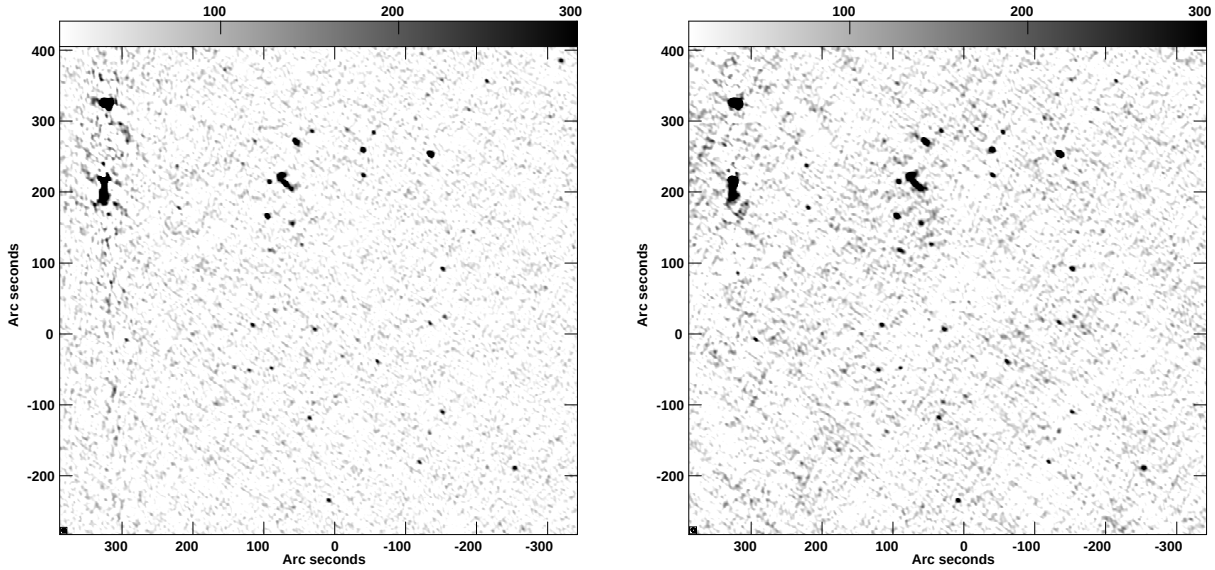

Figure 4: Image of Abell 2552 at 610 MHz obtained via two methods. The left panel image is from FLAGCAL data analysis and the right panel image is from the manual data analysis. (Credits: Dr. R. Kale.)

1.3.3 240 MHz

The imaging results at 240 MHz for the 0707+5002 (dirty image) and for the NGC 5044 (CLEAN image) at 235 MHz sources are presented in Fig. 7 and in Fig. 8, respectively.

An interesting source to discuss is the extended source (second source from the bottom, seen visually and showing diffuse extended features) in the 325 MHz map (Fig. 8), also detected at the 240 MHz. The source, NGC 5054, is the part of the group environment, the integrated flux densities being $S_{325\,\mathrm{MHz}}$ = 210 $\pm$4 mJy, and $S_{235\,\mathrm{MHz}}$ = 312 $\pm$9 mJy. These measurements form a straight-line radio spectra for the source giving a spectral index of 1.22 $\pm$0.04. An extrapolation to higher frequencies suggests the flux density at 1.49 GHz would be $\sim$35 $\pm$8 mJy for the source, which is consistent with the NED measurement of 43.2 mJy[4] within errorbars.

1.3.4 150 MHz

The imaging results at 150 MHz for the Abell 2256 source is presented in Fig. 9. It is a rich cluster of galaxies containing over 40 radio galaxies with fascinating observed properties across a range of wavelengths. Long believed to represent a cluster merger, in addition to the primary cluster and subcluster there is evidence for a third, poorer system.

This GMRT data at 150 MHz is one of the most challenging data! Although the observing band is protected, significant man-made RFI is present within the band at all times. In addition, the data are further complicated by ionospheric phase rotations that vary with time and viewing direction. In spite of these challenging issues, the FLAGCAL reduced image compares well with the manually reduced image, see Fig. 9 and Table 2 giving qualitative and quantitative levels of agreements. We compare further with the best map ever produced from this data using the technique of 'peeling' (SPAM:[5] Intema, private communication).

[4]NED: 1996, ApJS, 103, 81

[5]Intema et al. 2009, A&A, 501, 1185

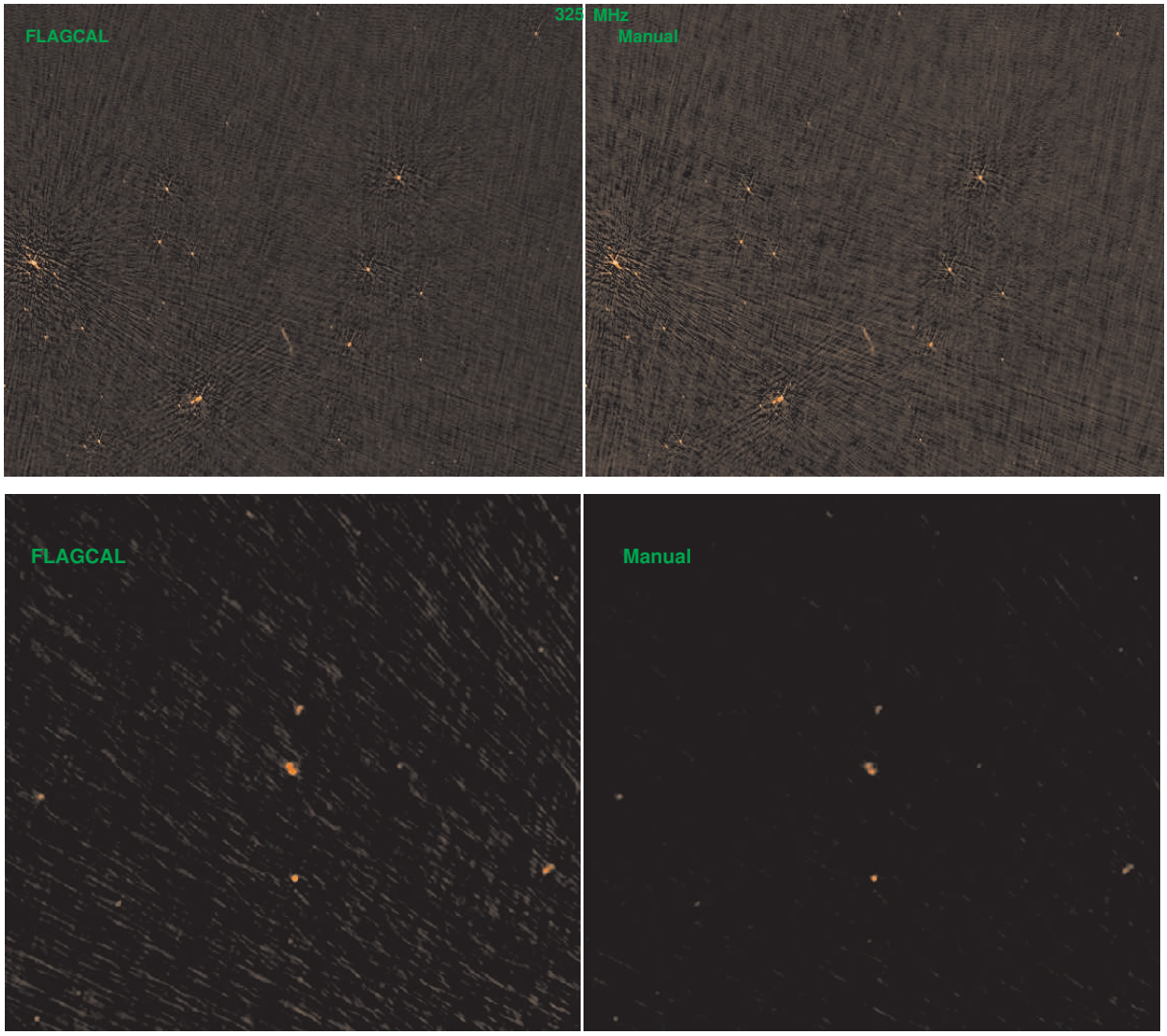

Figure 5: Images of Abell 3411 (upper-panel) and NGC 5044 (lower-panel) at 325 MHz obtained via two methods. The left panel is FLAGCAL image and the right panel is manually reduced image. Both images show a small part, $\sim$56 $\times$ 70 arcimn^2 (Abell 3411) and $\sim$33 $\times$ 31 arcimn^2 (NGC 5044) region from the mapped field-of-view. Peak surface brightnesses correspond to the peaks in the mapped fields-of-view, and the RMS' are determined from the empty regions in the mapped fields-of-view, which are listed in Table 2.

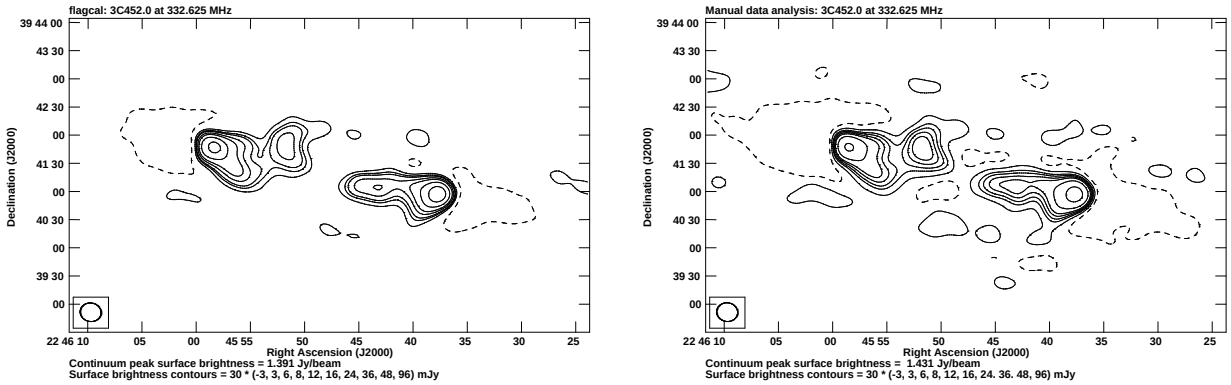

Figure 6: Image of 3C 452 at 325 MHz obtained via two methods. The left panel is FLAGCAL image and the right panel is manually reduced image. During imaging a UVTAPER of 10 kλ was applied to both methods in order to map diffuse, low surface brightness extended emission (reported by Sirothia et al. 2013 ApJ 765, L11); neither of the two efforts bring out this emission upto the quoted noise levels (see Table 2). Note the amazing positional agreements between the two images of various detected features, including radio core and hotspots.

This map made after correcting direction-dependent errors and solving for the ionosphere phase-screen has a peak flux density of 0.25 Jy and a RMS of 2.3 mJy beam^{-1}, where the beam is 49.0 $\times$ 23.7 arcsec^2 (= 70 pixels). This image morphologically and quantitatively compare within errorbars with the FLAGCAL and the manual outputs.

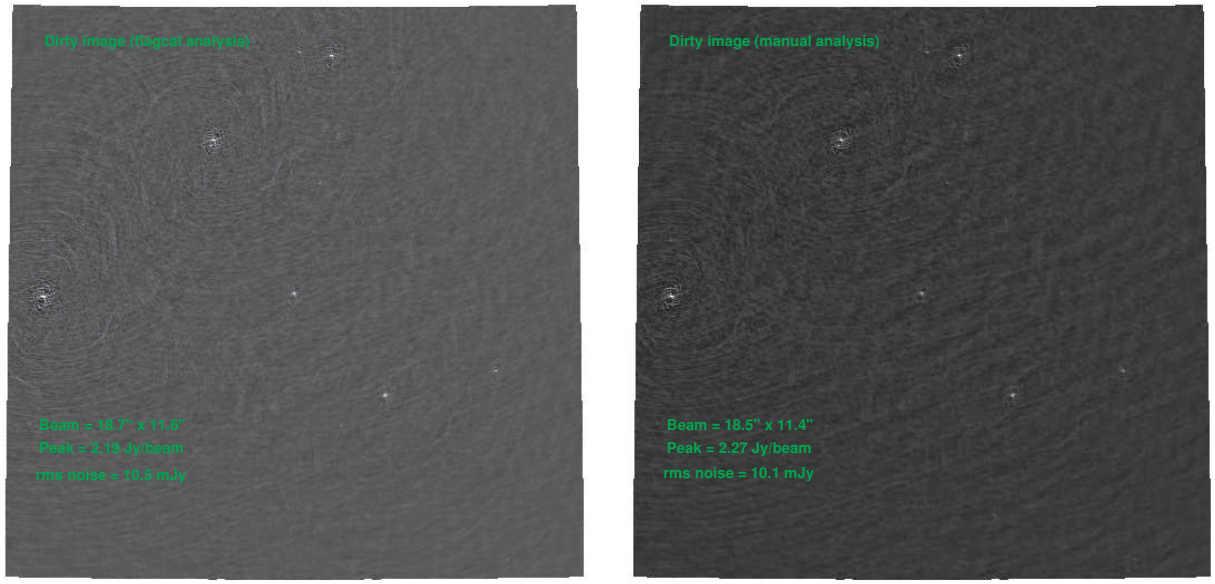

Figure 7: Image comparison from dirty images obtained via two methods for 0702+5002 source at 240 MHz. The left panel is FLAGCAL and the right panel is manually reduced image.

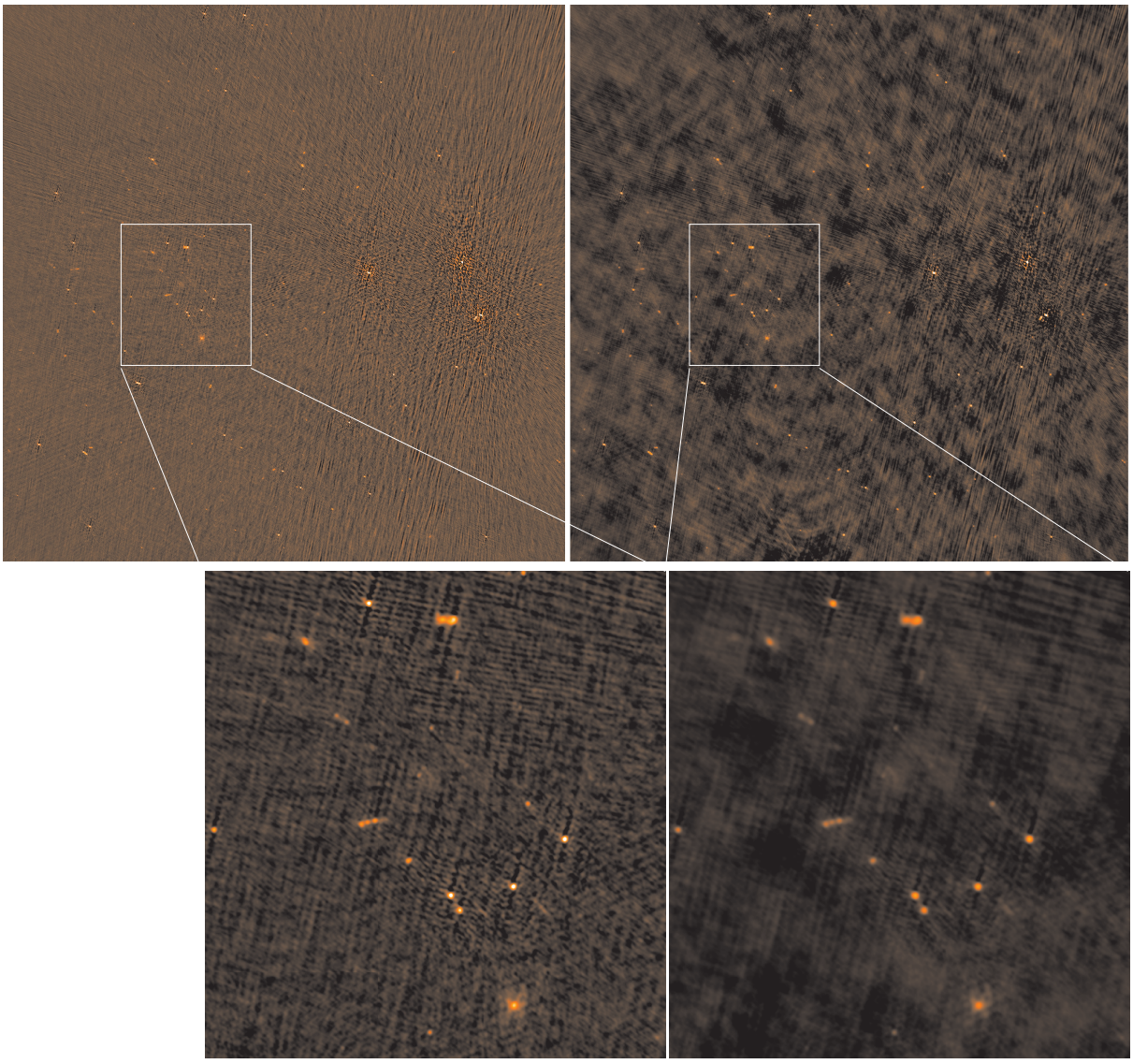

Figure 8: Image of NGC 5044 at 235 MHz obtained via two methods. Top panels show full FoVs and bottom panels show zoom of inner regions. The left panel is FLAGCAL and the right panel is manually reduced image.

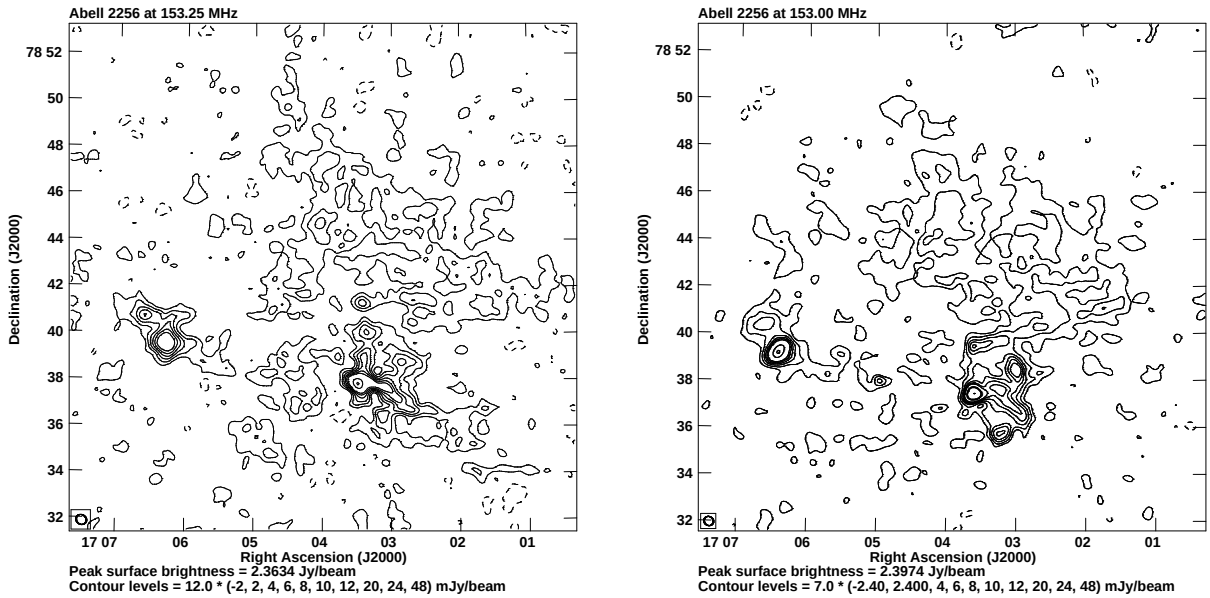

Figure 9: Image of Abell 2256 at 150 MHz obtained via two methods. On the left is FLAGCAL image and on the right is manually reduced image.

1.4 Summary

We have presented results from a FLAGCAL and manual data analysis study of several fields ranging from point source dominated to extdended source dominated fields, showing both low surface brightness diffuse structures and classical radio galaxies. Table 2 shows summary of results from the two methods.

The radio measurements presented here represent most of the database that we require for rigorously testing and understanding the FLAGCAL. Our conclusions from these new observations can be summarized as follows.

i The radio morphologies of the sources obtained via both, FLAGCAL and manual data reduction methodologies are largely identical with no visible artefacts, issues, etc.

ii In addition, as noted in Table 2, the quantitative comparisons of the two images, *i.e.*, the FLAGCAL and the manually reduced images, show fairly decent agreements within errorbars at all frequencies.

iii The flux densities of many field sources, both point and extended in our maps presented here, are consistent with the measurements from the literature.

iv Not only results from the CLEAN images, the dirty image of a simple field *e.g.*, 0707+5002 also shows remarkable morphological similarities and agreements in peak surface brightnesses, RMS noise levels, etc., in both the FLAGCAL and the manually reduced images.

v The morphology for Abell 2256 at 150 MHz obtained using FLAGCAL is largely consistent with the morphology obtained using manual data analysis. This is remarkable, because this field is rich, due to the existence of nearby galaxy cluster that has significant evidence of merger activity. In addition the map is dynamic range limited, the data suffers from ionospheric disturbances, etc. The best map ever produced from this data using the technique of 'peeling' (Intema, private communication) has a peak flux density of 0.25 Jy and a RMS of 2.3 mJy beam^{-1}, where the beam is 49.0 $\times$ 23.7 arcsec^2 (= 70 pixels).

vi Finally, the absolute positional accuracies in the maps presented here (from Fig. 2 to Fig. 9) obtained

via two methods also agree well. The uncertainties in peak positions of individual sources in the fields are well within the positional uncertainties in each of the two maps.

In short, the low-frequency radio maps presented above using FLAGCAL show morphologies that are similar to the morphologies obtained via. manual data analysis. The FLAGCAL analysed data and the mapping and measurement results show that, in general, we do not find any evidence that FLAGCAL is showing inconsistent flux density scales or showing imaging artefacts, etc.; instead we find consistent results at large.

As users, we intend to see the next released ver. of FLAGCAL addressing, solving and correcting for the (i) direction dependent effects: here, we mean a correction of beam model as a function of time during the observing run, which would aim to calibrate pointing effects as a function of time, and (ii) ionospheric disturbances. Former would eventually bring us close to high dynamic range imaging! Inclusion of these corrections in the FLAGCAL should improve an order of magnitude in the imaging results.

Acknowledgements

DVL thanks (i) Prof. J.N. Chengalur for the support, help, useful conversations and push, which has enabled me to bring this report to a completion, and (ii) Dr. S. Konar for her carefully reading the manuscript. We thank the staff of the GMRT that made these observations possible. GMRT is run by the National Centre for Radio Astrophysics of the Tata Institute of Fundamental Research.